Korean J. Chem. Eng., **26**(6), 1591-1600 (2009)
DOI: 10.1007/s11814-009-0341-1

Kinetic parameter estimation of the Fischer-Tropsch synthesis reaction on K/Fe-Cu-Al catalysts

Yun Ha Kim*,*, Du-Yeong Hwang**, Sang Hoon Song***, Sang Bong Lee***, Eun Duck Park*,***, and Myung-June Park**,†**

*Division of Energy Systems Research, Ajou University, Suwon 443-749, Korea
**Department of Chemical Engineering, Ajou University, Suwon 443-749, Korea
***Korea Research Institute of Chemical Technology, Daejeon 305-600, Korea
(*Received 17 June 2009 • accepted 16 July 2009*)

Abstract−This paper addresses the development of a mathematical model for a fixed-bed reactor where the Fischer-Tropsch synthesis reaction takes place. The model includes the consumption rate of carbon monoxide and the production rates for paraffin and olefin chains (up to the length of 47). The kinetic parameters are estimated using the experimental data under various experimental conditions with the effect of temperature, space velocity, the composition of feed mixture and pressure included. The simulation results with the estimated parameters predict the CO conversion, methane selectivity, paraffin selectivity and the entire distribution of hydrocarbon products satisfactorily. A further investigation on the effect of operating conditions shows that the ratio of hydrogen to carbon monoxide and the pressure are the effective variables for the determination of the entire distribution.

Key words: Fischer-Tropsch Synthesis, K/Fe-Cu-Al Catalyst, Mathematical Model, Fixed-bed Reactor, Entire Distribution, Hydrocarbon Products

INTRODUCTION

Fischer-Tropsch (FT) reaction is hard to predict due to its severe heat generation and complex reaction mechanism. Since the conversion and the selectivity to high value added chemicals are very low, the FT process has been commercialized in locations where the supply of crude oil is very limited. Due to the skyrocketing oil price, however, interest in the development of the liquid fuel production process has increased, and the reinforced environmental regulation necessitates the production of clean liquid fuel with lower sulfur content. Therefore, research effort has been focused on the development of XTL processes which are composed of the syngas (CO and H_2) generation and FT process.

FT reaction produces hydrocarbon chemicals from the syngas via the following main reaction pathways:

$$\text{Paraffin formation: } nCO+(2n+1)H_2 \rightarrow C_nH_{2n+2}+nH_2O \quad (1)$$

$$\text{Olefin formation: } nCO+2nH_2 \rightarrow C_nH_{2n}+nH_2O \quad (2)$$

It is well known that VIII group metals can be used as a catalyst for FT reaction [1,2]. As noble metals such as Rh, Ir, Pt and Pd are less reactive than non-noble metals such as Fe and Co, most of researches are conducted using Ru, Fe, Co and Ni, among which Ru and Ni are inadequate for the commercial processes because Ru is too expensive and Ni is transformed to nickel carbonyl form under high pressure conditions. Vannice [1] reported that the average molecular weights were decreased in the order of Ru>Fe>Co>Rh>Ni>Ir>Pt>Pd. The Fe-based catalyst is inexpensive compared to Co-based one and is known to be less sensitive to impurities included in the syngas (for example, sulfur). In addition, it can be applied to the process with low H_2/CO ratio. It is worth noting, however, that the deactivation proceeds more rapidly for Fe-based catalyst than Co-based one.

Zhao et al. [3] have shown that the catalyst system composed of FeMn-SiO_2 and K-Al_2O_3 has the highest CO conversion among mixed catalyst systems composed of FeMn-SiO_2 and various promoters such as K-Al_2O_3, K-SiO_2, K-ZSM-5 and K-free. Other than K [4], Cu [5] and Mn [6] were also suggested as a good candidate for the co-catalyst. On the basis of the above features, K/Fe-Cu-Al catalyst has been prepared and tested for the activity in this study.

Many research works have been conducted for the development of kinetics on Fe-based Fischer-Tropsch synthesis (FTS) reaction. However, since little is known about the detailed mechanism, no exact kinetic model has been developed yet. It is reported that the promoted Fe catalyst shows higher water-gas-shift (WGS) activity than unpromoted Fe catalyst [7], and the high WGS activity causes the increased rate of water consumption resulting in very little amount of water. In this case, the inhibition reaction by water can be neglected. Anderson [8] applied the Eley-Rideal mechanism for the kinetic rate by assuming competitive adsorption of CO and H_2O, and inhibition by water. This kinetics has been applied by other research workers [9,10], while Huff and Satterfield [11] developed the modified version where the hydrocarbon is produced via the reaction of hydrogen with the adsorbed carbon. With the additional assumption that the amount of water is negligible, the reaction rate becomes a first-order equation for the hydrogen while 0^{th} for carbon monoxide [12,13]. Meanwhile, Ledakowicz et al. [7] showed that the first-order equation for the hydrogen fails to fit the experimental data, and then developed the rate equations including the inhibition by carbon diox-

†To whom correspondence should be addressed.
E-mail: mjpark@ajou.ac.kr

ide. However, the reaction rates based on the simple mechanism are inappropriate for the complex multi-component mixtures by the FTS, and the distributions of paraffin and olefin are distinguished.

Recently, the reaction rates on the basis of more detailed kinetic mechanisms have been suggested to predict the distribution of paraffin and olefin products [14,15]. Lox and Froment [14] proposed five elementary reaction sets: (1) adsorption of carbon monoxide, (2) reaction of hydrogen, (3) formation of hydrocarbon building block "CH_2", (4) incorporation of the hydrocarbon building block with one carbon atom into a hydrocarbon intermediate with one and more carbon atoms, and (5) desorption of hydrocarbon products. Wang et al. [15] augmented the re-adsorption of olefins based on the experimental results [15-17].

In this study, the activity of K/Fe-Cu-Al is evaluated by using a lab-scale fixed bed reactor under a variety of conditions, in such a way that the effect of operating conditions on the distribution of hydrocarbon product is discussed. Reaction rates by Wang et al. [15] are applied to a plug flow reactor model and experimental data are used to estimate the effective kinetic parameters.

EXPERIMENTAL

1. Preparation of Catalysts

Fe-Cu-Al was first prepared by a co-precipitation method. The pH of the aqueous solution of $Fe(NO_3)_3 \cdot 9H_2O$, $Cu(NO_3)_2 \cdot 3H_2O$ and $Al(NO_3)_3 \cdot 9H_2O$ was increased to be 7 by adding 0.5 M NH_4OH solution. The slurry was aged at 353 K for 1 h, filtered, and dried at 383 K for 1 day. After adding excess amounts of the aqueous K_2CO_3 solution on Fe-Cu-Al just dried at 383 K for 1 day, the liquid water was evaporated and the catalyst was dried at 383 K for 2 days. This impregnated catalyst was calcined in air at 723 K for 5 h and reduced in H_2 at 673 K for 6 h before a reaction. The K/Fe/Cu/Al mole ratio was 4/100/6/16.

2. Activity Test

Catalyst activity and kinetic tests were carried out in a small fixed bed reactor with catalysts that had been retained between 45 and 80 mesh sieves (*cf.* Fig. 1 for the scheme of experimental setup). For all experiments, catalyst without diluents was contacted with various conditions and Ar was used as the standard gas. Activity and selectivity measurements were conducted in conditions such as 5-20 bar total pressure, 503-523 K, H_2/CO ratios of 0.5-2 and 1,500-2,300 h^{-1} space velocities. The detailed description of experimental conditions can be found in Table 1. The effluent gas composition was determined through gas chromatographic analysis (M600D) with a thermal conductivity detector (TCD, carbosphere column) and a flame ionization detector (FID, poraplot Q column). The CO conversion, CO_2 selectivity, hydrocarbon (HC) selectivity, CH_4 selectivity, C2-C4 selectivity and C5+ selectivity were calculated by using the following formulas:

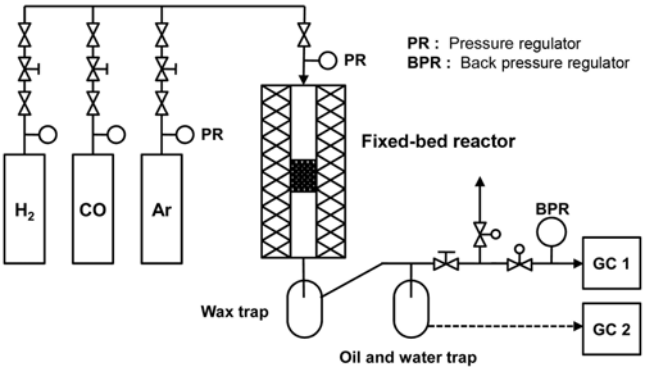

Fig. 1. The experimental setup for the Fischer-Tropsch synthesis reaction over Fe-based catalyst.

Table 1. Experimental conditions

Case number	Temperature [K]	SV [h^{-1}]	H_2/CO ratio	Pressure [bar]	Remarks
1	503	1500	2	10	SV
2	503	1900	2	10	
3	503	2300	1.5	10	H_2/CO ratio
4	503	2300	2	10	Ref. at 503 K
5	513	2300	1	10	H_2/CO ratio
6	513	2300	1.5	10	
7	513	2300	2	5	Pressure
8	513	2300	2	10	Ref. at 513 K
9	513	2300	2	15	Pressure
10	513	2300	2	20	
11	523	2300	0.5	10	H_2/CO ratio
12	523	2300	1	10	
13	523	2300	1.5	10	
14	523	2300	2	10	Ref. at 523 K

$$\text{CO conversion } (\%) = \frac{[CO]_{in} - [CO]_{out}}{[CO]_{in}} \times 100 \quad (3)$$

$$CO_2 \text{ selectivity } (\%) = \frac{[CO_2]_{out}}{[CO]_{in} - [CO]_{out}} \times 100 \quad (4)$$

$$\text{HC selectivity } (\%) = \frac{[CO]_{in} - [CO]_{out} - [CO_2]_{out}}{[CO]_{in} - [CO]_{out}} \times 100 \quad (5)$$

$$CH_4 \text{ selectivity } (\%) = \frac{[CH_4]_{out}}{[CO]_{in} - [CO]_{out} - [CO_2]_{out}} \times 100 \quad (6)$$

$$\text{C2-C4 selectivity } (\%) = \frac{\sum_{i=2}^{4} i(C_iH_{2i} + C_iH_{2i+2})}{[CO]_{in} - [CO]_{out} - [CO_2]_{out}} \times 100 \quad (7)$$

$$\text{C5+ selectivity } (\%) = \frac{[HC]_{out} - [CH_4]_{out} - \sum_{i=2}^{4} i(C_iH_{2i} + C_iH_{2i+2})}{[HC]_{out}} \times 100 \quad (8)$$

And the liquid products were analyzed through gas chromatographic analysis (HP 6890) with an FID (HP-5 column).

MATHEMATICAL MODEL

Wang et al. [15] proposed a detailed reaction mechanism for Fischer-Tropsch synthesis (FTS) over an industrial Fe-Cu-K catalyst, where the olefin re-adsorption mechanism has been additionally augmented to the kinetics proposed by Lox and Froment [14]. The assumptions include different sites for FTS reactions and water gas

Table 2. Elementary steps for FTS reaction [15]

No.	Elementary reaction of FTS	Expression of rates or equilibrium constants
S0	$H_2 + 2\kappa \leftrightarrow 2H\cdot\kappa$	$K_0 = \frac{[H\cdot\kappa]^2}{P_{H_2}[\kappa]^2}$
S1	$H\cdot\kappa + CO \leftrightarrow H\cdot\kappa\cdot CO$	$r_{0,1} = k_1 P_{CO}[H\cdot\kappa]$
S2	$H\cdot\kappa\cdot CO + H_2 \leftrightarrow H\cdot\kappa\cdot C + H_2O$	$K_2 = \frac{[H\cdot\kappa\cdot C]P_{H_2O}}{[H\cdot\kappa\cdot CO]P_{H_2}}$
S3	$H\cdot\kappa\cdot C + H_2 \leftrightarrow H\cdot\kappa\cdot CH_2$	$K_3 = \frac{[H\cdot\kappa\cdot CH_2]}{[H\cdot\kappa\cdot C]P_{H_2}}$
S4	$H\cdot\kappa\cdot C_2 \leftrightarrow CH_3\cdot\kappa$	$K_4 = \frac{[CH_3\cdot\kappa]}{[H\cdot\kappa\cdot CH_2]}$
S5	$CH_3\cdot\kappa + H_2 \leftrightarrow CH_4 + H\cdot\kappa$	$r_{1,5} = k_{5M} P_{H_2}[CH_3\cdot\kappa]$
	⋮	
S1	$C_{n-1}H_{2n-1}\cdot\kappa + CO \leftrightarrow C_{n-1}H_{2n-1}\cdot\kappa\cdot CO$	$r_{n-1,1} = k_1 P_{CO}[C_{n-1}H_{2n-1}\cdot\kappa]$
S2	$C_{n-1}H_{2n-1}\cdot\kappa\cdot CO + H_2 \leftrightarrow C_{n-1}H_{2n-1}\cdot\kappa\cdot C + H_2O$	$K_2 = \frac{[C_{n-1}H_{2n-1}\cdot\kappa\cdot C]P_{H_2O}}{[C_{n-1}H_{2n-1}\cdot\kappa\cdot CO]P_{H_2}}$
S3	$C_{n-1}H_{2n-1}\cdot\kappa\cdot C + H_2 \leftrightarrow C_{n-1}H_{2n-1}\cdot\kappa\cdot CH_2$	$K_3 = \frac{[C_{n-1}H_{2n-1}\cdot\kappa\cdot CH_2]}{[C_{n-1}H_{2n-1}\cdot\kappa\cdot C]P_{H_2}}$
S4	$C_{n-1}H_{2n-1}\cdot\kappa\cdot CH_2 \leftrightarrow C_nH_{2n+1}\cdot\kappa$	$K_4 = \frac{[C_nH_{2n+1}\cdot\kappa]}{[C_{n-1}H_{2n-1}\cdot\kappa\cdot CH_2]}$
S5	$C_{n-1}H_{2n+1}\cdot\kappa\cdot H_2 \leftrightarrow C_nH_{2n+2} + H\cdot\kappa$	$r_{n,5} = k_5 P_{H_2}[C_nH_{2n+1}\cdot\kappa]$
S6	$C_nH_{2n+1}\cdot\kappa \leftrightarrow C_nH_{2n} + H\cdot\kappa$	$r_{n,6} = k_6[C_nH_{2n+1}\cdot\kappa] - k_{-6}P_{C_nH_{2n}}[H\cdot\kappa]$

shift (WGS) reaction, and carbide polymerization mechanism and formate mechanism for FTS and WGS reactions, respectively. In their work, the rate determining steps (RDS) for FTS reactions were determined as both the adsorption of CO and the desorption of hydrocarbon products, while the desorption of gaseous carbon dioxide via formate intermediate species was shown to be an RDS for the WGS reaction. In this study, the reaction mechanism proposed by Wang et al. [15] are used and the elementary reaction steps are presented in Table 2. The details about the development of reaction rates are referred to the Wang et al. [15], while the resulting reaction rates are summarized as follows:

$$R_{CH_4} = k_{5M}P_{H_2}\alpha_1 / \left\{ 1 + \left(1 + \frac{1}{K_2K_3K_4}\frac{P_{H_2O}}{P_{H_2}^2} + \frac{1}{K_3K_4}\frac{1}{P_{H_2}} + \frac{1}{K_4}\right)\sum_{i=1}^{N}\left(\prod_{j=1}^{i}\alpha_j\right)\right\} \quad (9)$$

$$R_{C_nH_{2n+2}} = k_5 P_{H_2}\prod_{j=1}^{n}\alpha_j / \left\{ 1 + \left(1 + \frac{1}{K_2K_3K_4}\frac{P_{H_2O}}{P_{H_2}^2} + \frac{1}{K_3K_4}\frac{1}{P_{H_2}} + \frac{1}{K_4}\right)\sum_{i=1}^{N}\left(\prod_{j=1}^{i}\alpha_j\right)\right\} \quad (n\geq 2) \quad (10)$$

$$R_{C_nH_{2n}} = k_6(1-\beta_n)\prod_{j=1}^{n}\alpha_j / \left\{ 1 + \left(1 + \frac{1}{K_2K_3K_4}\frac{P_{H_2O}}{P_{H_2}^2} + \frac{1}{K_3K_4}\frac{1}{P_{H_2}} + \frac{1}{K_4}\right)\sum_{i=1}^{N}\left(\prod_{j=1}^{i}\alpha_j\right)\right\} \quad (n\geq 2) \quad (11)$$

$$R_{CO_2} = \frac{k_y(P_{CO}P_{H_2O}/P_{H_2}^{0.5} - P_{CO_2}P_{H_2}^{0.5}/K_P)}{1 + K_yP_{CO}P_{H_2O}/P_{H_2}^{0.5}} \quad (12)$$

where

$$\alpha_1 = k_1P_{CO}/(k_1P_{CO} + k_{5M}P_{H_2}) \quad (13)$$

$$\alpha_A = k_1P_{CO}/(k_1P_{CO} + k_5P_{H_2} + k_6) \quad (14)$$

$$\alpha_n = k_1P_{CO}/\{k_1P_{CO} + k_5P_{H_2} + k_6(1-\beta_n)\} \quad (15)$$

$$\beta_n = \frac{k_{-6}}{k_6}\frac{P_{C_nH_{2n}}}{\alpha_A^{n-1}\frac{k_1P_{CO}}{k_1P_{CO}+k_5P_{H_2}} + \frac{k_{-6}}{k_1P_{CO}+k_5P_{H_2}+k_6}\sum_{h=2}^{n}(\alpha_A^{h-1}P_{C_{(n-h+2)}H_{2(n-h+2)}})} \quad (16)$$

It is assumed that the maximum chain length of hydrocarbons is 47 and water-gas-shift (WGS) reaction equilibrium constant (K_p) is specified as follows [18]:

$$\ln K_P = \frac{5078.0}{T} - 5.9 + (1.4\times10^{-5}T) - (2.8\times10^{-9}T^2) \quad (17)$$

Since the L-to-D ratio of a lab-scale fixed-bed reactor used in the experiments is very large and the mass transfer resistance is neglected due to the small size of the catalyst particle, one-dimensional pseudo-homogeneous plug flow reactor model is used to simulate the reactor as follows:

$$\text{Mass balance: } \frac{d(u_sc_i)}{dz} - \rho_B\sum_{j=1}^{NR}\alpha_{i,j}R_j = 0 \quad (18)$$

$$\text{Energy balance: } \frac{d(u_sC_P\rho_gT)}{dz} = \rho_B\sum_{j=1}^{NR}(-\Delta H)_jR_j + \frac{4U}{D_t}(T_W - T) \quad (19)$$

$$\text{Boundary conditions: } c_i = c_{i,0};\ T = T_{in} \text{ at } z = 0 \quad (20)$$

Here, u_s, ρ_B, ρ_g, R_j, and $\alpha_{i,j}$ represent the linear velocity, bulk and gas densities, reaction rate and stoichiometric coefficient, respectively, and other symbols are referred to the 'Nomenclature'. Heat capacity (C_p) and reaction enthalpy for the reaction j (ΔH_j) are assumed to be constant, and thus the values at 513 K have been used. The values of C_p, ΔH_j and gas density of component i ($\rho_{g,i}$) are available in a process simulator (UniSim Design Suite, Honeywell Inc.).

It is worth noting that the occurrence of any internal pore diffusion limitation is determined on the basis of the Weisz-Prater criterion, where the dimensionless Weisz-Prater parameter (C_{WP}) is calculated as follows:

$$C_{WP} = \frac{-r_{A,obs}\rho_c R_c^2}{D_{eff} C_A} \tag{21}$$

where $-r_{A,obs}$ is the rate of the reaction in mol/kg of catalyst/s and ρ_c is the catalyst density in kg/m^3. R_c, D_{eff}, and C_A represent the effective radius of the catalyst (the ratio of catalyst pellet volume to the surface area of catalyst) in m, the effective diffusivity in m^2/s and the limiting reactant concentration in the mixture in mol/cm^3, respectively. If the C_{WP} is much greater than unity, a strong resistance to internal pore diffusion exists, resulting in a concentration gradient from the catalyst surface to its pores [19]. Since the values of C_{WP} for all experimental conditions are calculated lower than 0.01, it is assumed that there is no internal diffusion limitation.

RESULTS AND DISCUSSION

1. Parameter Estimation

To estimate kinetic parameters, hydrocarbons with their chain length between 8 and 47 (C_8-C_{47}) were taken into account because carbon numbers higher than 10 are of interest in this study. In addition, the CO conversion, CH_4 selectivity (*cf.* Eq. (6)) and paraffin selectivity (fraction of paraffins over total amount of hydrocarbons) were included in the estimation and, thus, the following objective function was defined:

$$F_{obj} = \frac{1}{2}\sum \left\{ \begin{array}{l} \left(w_1 \frac{P_{n,calc} - P_{n,exp}}{P_{n,exp}}\right)^2 + \left(w_1 \frac{P_{w,calc} - P_{w,exp}}{P_{w,exp}}\right)^2 \\ + \left(w_2 \frac{O_{n,calc} - O_{n,exp}}{O_{n,exp}}\right)^2 + \left(w_2 \frac{O_{w,calc} - O_{w,exp}}{O_{w,\exp}}\right)^2 \\ + \left(w_3 \frac{X_{calc} - X_{exp}}{X_{exp}}\right)^2 + \left(w_4 \frac{S_{CH_4,calc} - S_{CH_4,exp}}{S_{CH_4,exp}}\right)^2 \\ + \left(w_5 \frac{S_{P,calc} - S_{P,exp}}{S_{P,exp}}\right)^2 \end{array} \right\} \tag{22}$$

where P_n/P_w and O_n/O_w represent the number-/weight-averaged chain length of paraffins and olefins, respectively, while X, S_{CH_4}, and S_P denote the CO conversion, methane selectivity and paraffin selectivity at the exit of the reactor, respectively. Subscripts 'calc' and 'exp' mean the calculated and experimental values, respectively, and w_i is a weighting factor.

The temperature dependence of kinetic parameters is as follows:

$$k_i(T) = k_{i,0}\exp\left[-\frac{E_i}{R}\left(\frac{1}{T} - \frac{1}{T_0}\right)\right] \tag{23}$$

$$K_i(T) = K_{i,0}\exp\left[\frac{-\Delta H_i}{R}\left(\frac{1}{T} - \frac{1}{T_0}\right)\right] \tag{24}$$

The parameters ($k_{i,0}$ and $K_{i,0}$) at the reference temperature, activation energies, and enthalpies are scaled in the form of $y_{scaled} = y_{actual}/y_{scaling\text{-}factor}$ in order to reduce the statistical correlation and to prevent the ill-conditioning problems resulting from the differences of the orders of magnitude between parameters. The reference temperature (T_0) is specified as 513 K.

Since each experimental condition produces seven data points (CO conversion, methane selectivity, paraffin selectivity, two types

Table 3. Estimated values of kinetic parameters

Parameter	Dimension	Estimate	Note
$k_{1,0}$	mol/(g·s·bar)	4.78×10^{5}	CO adsorption
E_1	J/mol	1.09×10^{5}	
$k_{5M,0}$	mol/(g·s·bar)	2.24×10^{2}	Methane formation
E_{5M}	J/mol	8.38×10^{4}	
$k_{5,0}$	mol/(g·s·bar)	1.09×10^{7}	Paraffin formation
E_5	J/mol	1.34×10^{5}	
$k_{6,0}$	mol/(g·s)	1.78×10^{7}	Olefin desorption reaction
E_6	J/mol	1.29×10^{5}	
$k_{v,0}$	mol/(g·s·bar$^{1.5}$)	1.71×10^{-4}	CO_2 formation (WGSR)
E_v	J/mol	2.61×10^{4}	
$k_{-6,0}$	mol/(g·s·bar)	3.12×10^{-4}	Olefin re-adsorption reaction
E_{-6}	J/mol	1.11×10^{4}	
K_v	bar$^{-0.5}$	3.03×10^{-1}	Group of constants in WGSR
$K_{2,0}$	-	2.14×10^{-10}	The hydrogenation of the adsorbed CO
$-\Delta H_2$	J/mol	7.24×10^{4}	
$K_{3,0}$	-	1.53×10^{-2}	The hydrogenation of H-κ-C
$-\Delta H_3$	J/mol	2.39×10^{4}	
$K_{4,0}$	-	9.33×10^{-2}	The hydrogenation of H-κ-CH_2
$-\Delta H_4$	J/mol	1.56×10^{4}	

of average chain lengths for paraffin and olefin) and the number of experimental condition is 14, total 98 points are used in the nonlinear data-fitting procedure. The objective function, Eq. (22), is minimized by using the *lsqcurvefit* subroutine in the MATLAB (The MathWorks, Inc.) where the Levenberg-Marquardt method is applied.

The numerical integration of Eqs. (18) and (19), which is required during each iterative step in the nonlinear regression, is performed by the ODE solver, *ode15s* implemented in the MATLAB. It is noted that the state variables of ODE's are also scaled using the value under a reference condition (condition number 8 in Table 1) to avoid ill-conditioning.

2. Estimation Results and Discussion

Table 3 shows the estimated values of kinetic parameters in this study. All the weighting factors for the components of the objective function are specified as unity. The rate constants for the CO adsorption (k_1) and olefin re-adsorption reaction (k_{-6}), and the equilibrium constants for the hydrogenation of the adsorbed CO (K_2), the hydrogenation of H-κ-C (K_3) and the hydrogenation of H-κ-CH_2 (K_4) are estimated in the function of the temperature to improve the performance of the estimation, while they are fixed at constant values in Wang et al.'s work [15]. It should be noted that the activation energy of paraffin formation (*cf.* E_5 in Table 3) is lower than that of olefin desorption reaction (*cf.* E_6 in Table 3) [14,15]. For paraffin formation, the values reported in the literature are between 80 and 95 kJ/mol [14,15,20,21] and it is determined as 134 kJ/mol in our study. The activation energy for the olefin desorption reaction in our study is 129 kJ/mol, which is similar to the values of 111.04 kJ/mol [15] and 132.3 kJ/mol [14]. However, the other parameters have been estimated within the range of physico-chemically reasonable values.

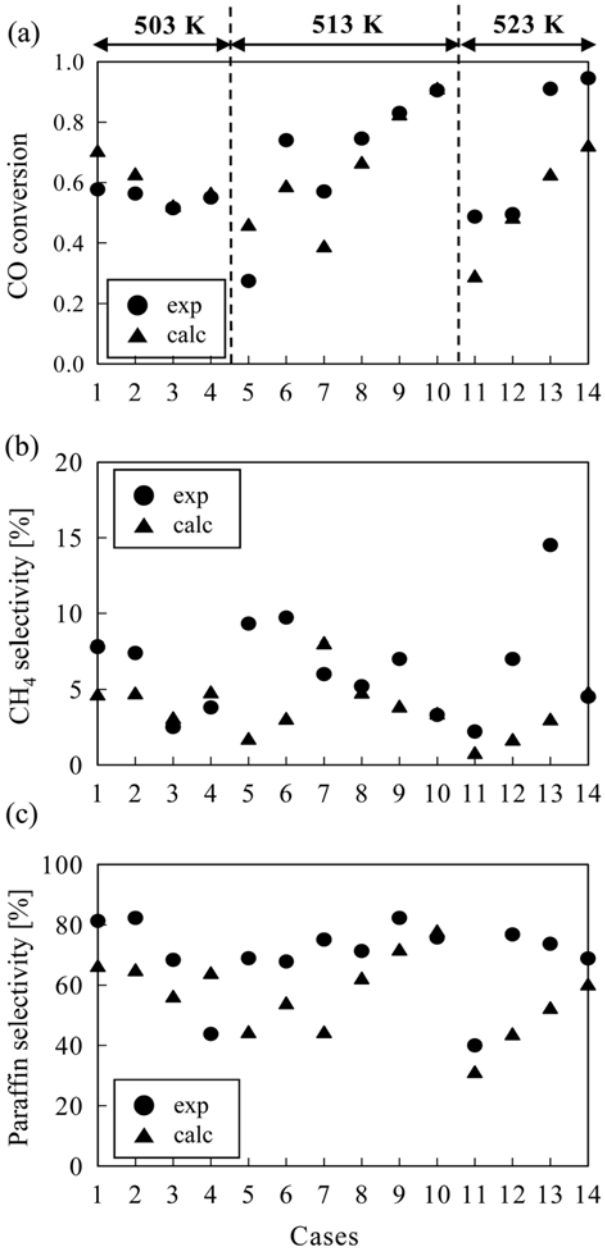

Fig. 2. Comparison of (a) CO conversion, (b) CH_4 selectivity, and (c) paraffin selectivity between the experimental data and the simulation values with the estimated kinetic parameters.

Fig. 2 shows the comparison of CO conversion, methane selectivity and paraffin selectivity between the experimental data and the simulation data using the estimated kinetic parameters. It is shown that the predictions by simulation are in good agreement with the experimental data. The average error defined as T.avg.error [%]=$\sum_i |(y_{i,exp}-y_{i,calc})/y_{i,exp}|\times 100$ is 19.08%, 42.44%, and 24.43% for CO conversion, methane selectivity and paraffin selectivity, respectively while the standard deviation of errors [%] is 19.25%, 29.01%, and 13.03%.

The calculated values of the number- and weight-averaged chain length of hydrocarbon products are shown in Fig. 3 with the experimental data. Weight-averaged values are fitted to the data very well, while little deviation is observed for number-averaged chain length. However, it can be seen that the model can predict the entire distributions of hydrocarbon products satisfactorily under most experimental conditions (*cf.* Diagrams (a) to (d) in Figs. 4, 5, 7 and 8). The average errors are 16.82%, 16.91%, 11.22% and 17.54% for P_n, P_w, O_n, and O_w, respectively, and their corresponding standard deviations of errors are 10.75%, 10.51%, 6.60% and 13.15%.

The effect of temperature, space velocity, feed ratio and pressure on the product distribution can be evaluated from the experimental data and the simulation results. On the basis of experimental results, the effects of operating conditions, when they are increased from the reference condition, on the properties of hydrocarbon products are summarized in Table 4.

When the temperature is increased, diagram (e) of Fig. 4 shows that the CO conversion at the exit of the reactor is increased because of the increased reaction rate resulting from the increased temperature inside the reactor (*cf.* Diagram (f) of Fig. 4). In the case of average chain length, high temperature leads to the decrease of chain length (*cf.* Diagrams (b) and (d) of Fig. 4). As a result, the fraction of gasoline (C5-C11) is increased while those of diesel (C12-C18) and wax (>C24) are decreased. The selectivity of C5+ is decreased as shown in Table 4.

The effect of the space velocity (SV) is shown in Fig. 5. The space velocity (SV), which is defined as the ratio of flow-rate to catalyst weight, is varied by adjusting the catalyst weight and fixing the flow-rate. Therefore, the increased space velocity (*i.e.*, the decreased amount of catalyst weight) corresponds to the short packing depth. As shown

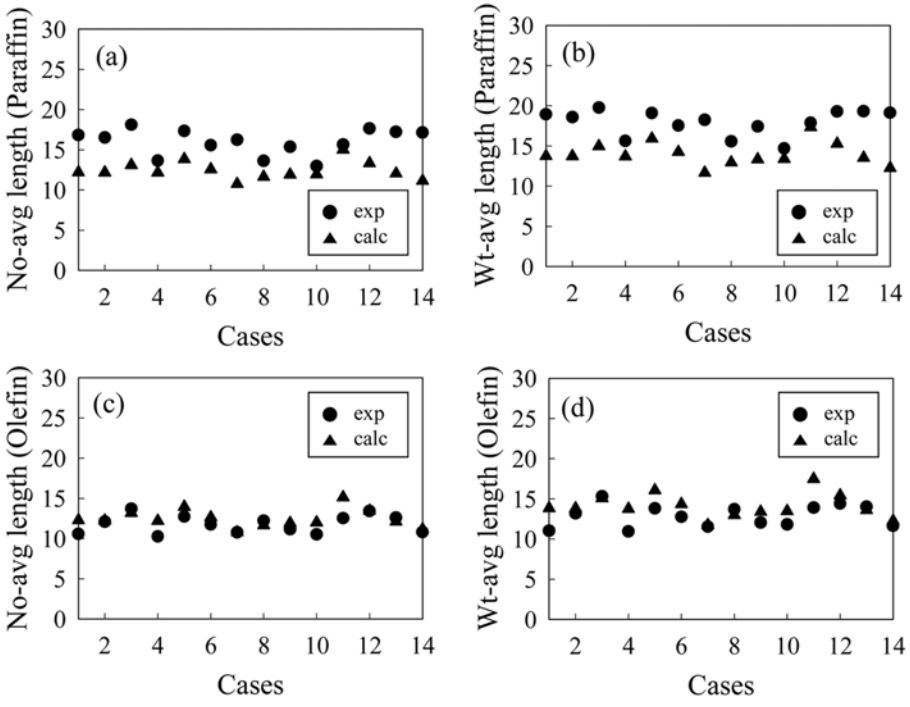

Fig. 3. Comparison of (a) number- and (b) weight-averaged length of paraffins, and (c) number- and (d) weight-averaged length of olefins between the experimental data and the simulation values with the estimated kinetic parameters.

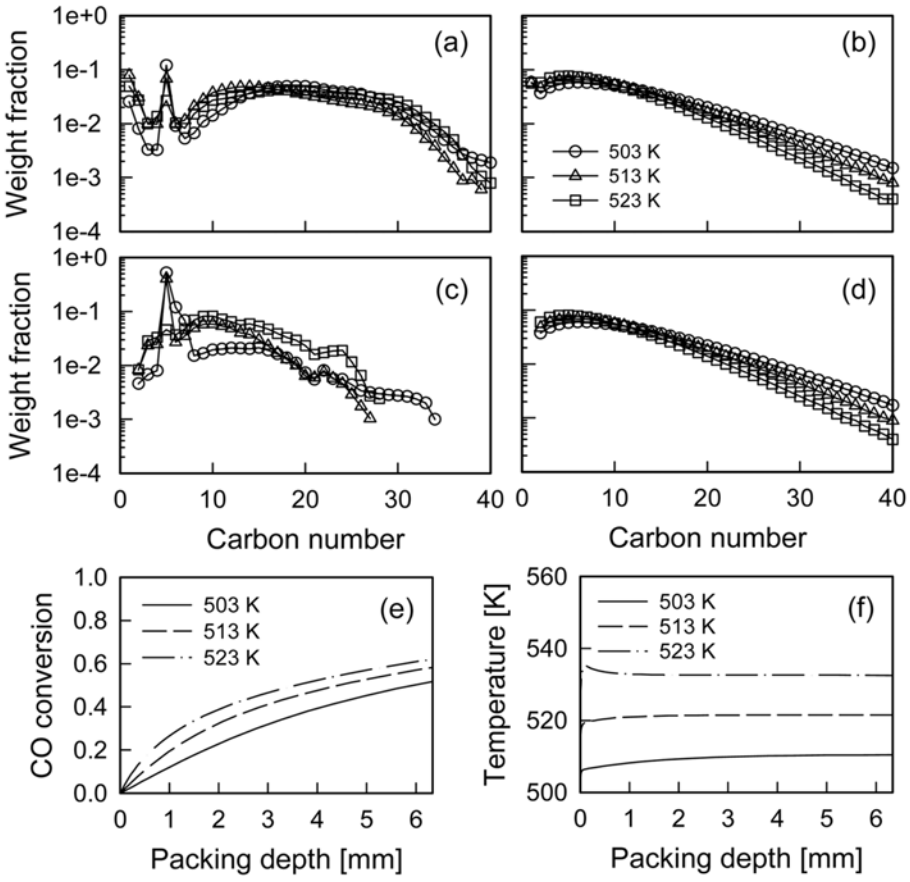

Fig. 4. The entire distribution of hydrocarbon products when the temperature is varied with P=10 bar, H_2/CO=1.5, and SV=2,300 h^{-1}. (a) Experimental data and (b) simulation values for paraffins; (c) experimental data and (d) simulation values for olefins; the evolution of (e) CO conversion and (f) temperature over the reactor axis (simulation results).

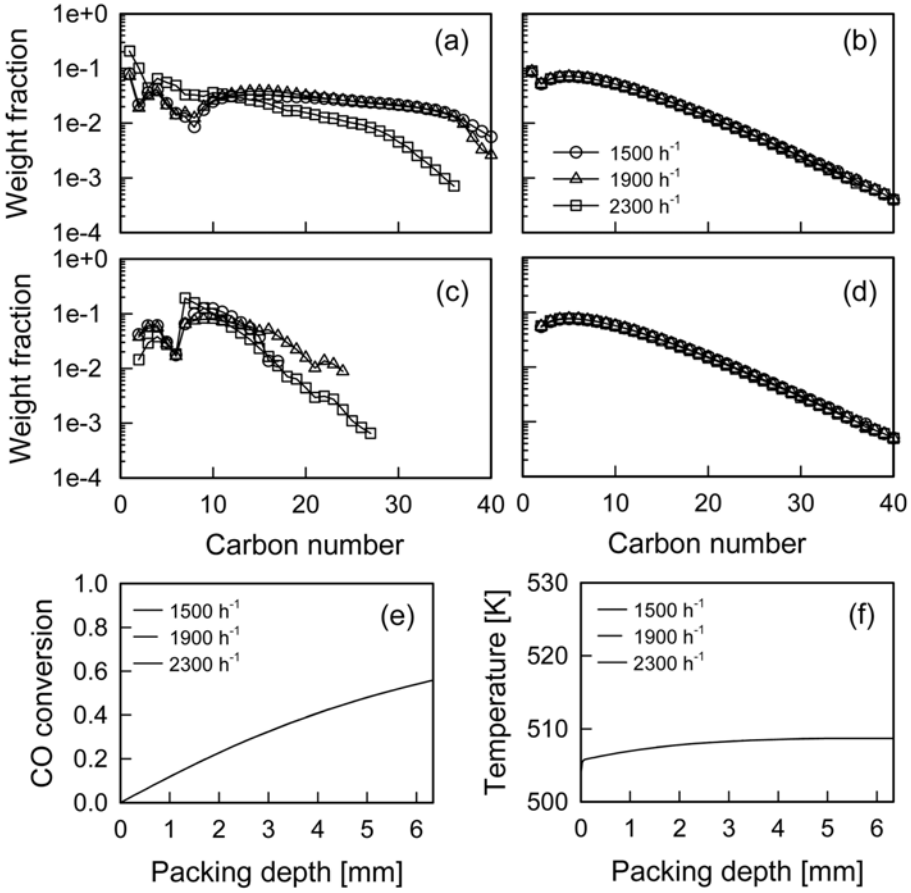

Fig. 5. The entire distribution of hydrocarbon products when the space velocity is varied with T=503 K, P=10 bar, and H_2/CO=1.5. (a) Experimental data and (b) simulation values for paraffins; (c) experimental data and (d) simulation values for olefins; the evolution of (e) CO conversion and (f) temperature over the reactor axis (simulation results).

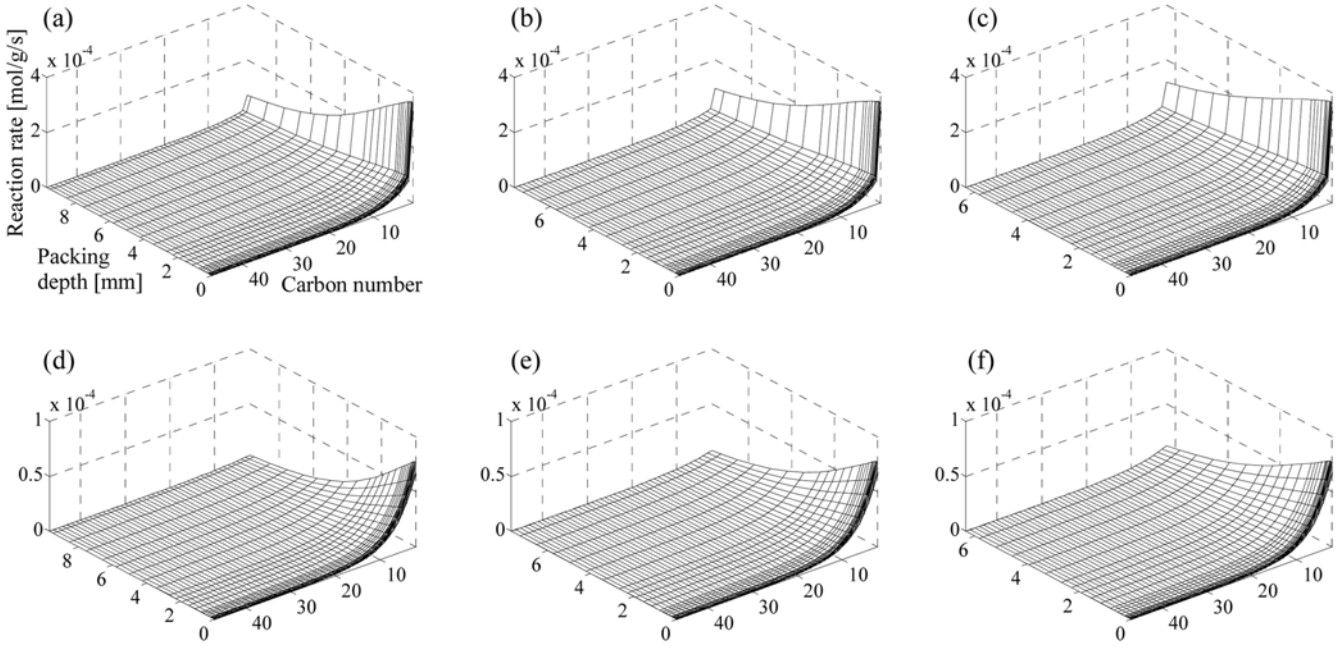

Fig. 6. The reaction rates of hydrocarbon with each chain length over the reactor axis when the space velocity is varied with T=503 K, P=10 bar, and H_2/CO=1.5. The values of SV are (a) 1,500 h^{-1}, (b) 1,900 h^{-1} and (c) 2,300 h^{-1} for paraffins, and (d) 1,500 h^{-1}, (b) 1,900 h^{-1} and (c) 2,300 h^{-1} for olefins.

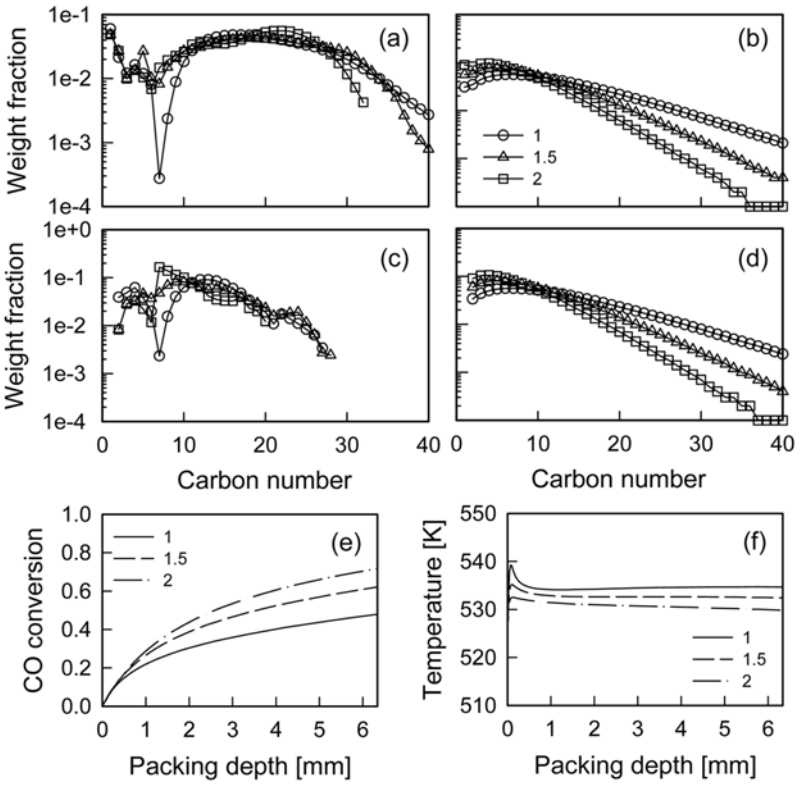

Fig. 7. The entire distribution of hydrocarbon products when the H_2/CO is varied with T=523 K, P=10 bar, and SV=2,300 h^{-1}. (a) Experimental data and (b) simulation values for paraffins; (c) experimental data and (d) simulation values for olefins; the evolution of (e) CO conversion and (f) temperature over the reactor axis (simulation results).

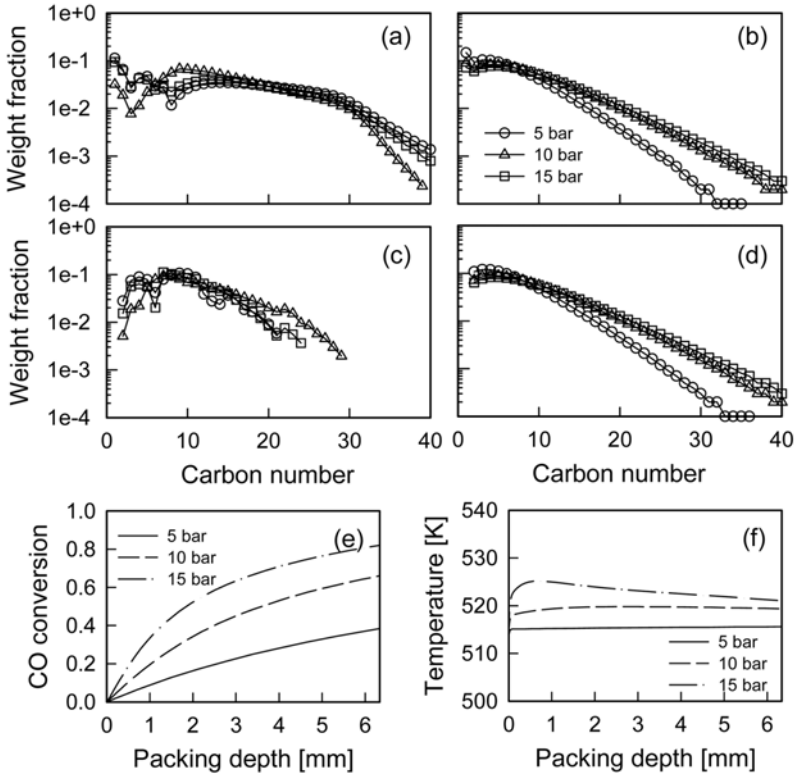

Fig. 8. The entire distribution of hydrocarbon products when the pressure is varied with T=513 K, H_2/CO=2, and SV=2,300 h^{-1}. (a) Experimental data and (b) simulation values for paraffins; (c) experimental data and (d) simulation values for olefins; the evolution of (e) CO conversion and (f) temperature over the reactor axis (simulation results).

Table 4. Effect of operating conditions on the conversion and the distribution hydrocarbon products

	CO conversion (C-mol%)	Selectivity (C-mol%)					O/(O+P) in C2-C4
		CO_2	HC	CH_4	C2-C4	C5+	
Temp.	↑	↑	↓	↑	↑	↓	↓
SV	↓	↓	↑	↓	↓	↓	↑
H_2/CO	↑	*	*	*	*	*	*
Pressure	↑	↑	↓	↓	↓	↑	↓

↑ and ↓ represent the increase and the decrease, respectively, while * means the complex behavior

in the diagrams (a) to (d), the entire distributions of hydrocarbon products under different SV's are overlapped. This is because the conditions of same flow rates result in the same profile of reaction rates along the reactor axis; this feature can be observed in Fig. 6, where the evolution of reaction rates along the reactor axis is provided. It is shown that the shape of the reaction rates curve at the inlet of the reactor is maintained until the exit of the reactor (see the locus of peak reaction rate along the reactor axis is unchanged).

The ratio of hydrogen to carbon monoxide influences the reactor dynamics and product qualities significantly. As shown in Fig. 7, the increased ratio results in increased CO conversion and decreased peak temperature, when total flow rate is unchanged. However, the values of yield (inlet CO molar flow rate times CO conversion) are almost equal for different ratio (9.67e-5 mol/min for H_2/CO=1; 9.64e-5 mol/min for H_2/CO=2). In other words, one can expect a safer operating environment if the ratio of H_2 to CO is increased, in the sense of operating temperature. In addition, the benefit of increased hydrogen amount is observed in the distribution of hydrocarbon products. Since the amount of wax is decreased with increasing hydrogen ratio, the load in the post-process (that is, hydro-cracking process) is diminished and a clogging problem may not take place in a relatively narrow tube reactor as well as a pipe.

The effect of pressure is also significant. The increased pressure results in the increased CO conversion, but the peak temperature is increased. It is shown that the fractions of oil and wax are increased at the same time. In conclusion, the change of pressure is effective for the increased production of oil, but the increased amount of wax and the high peak temperature may cause several problems in large-scale production.

It is worth noting that, under all experimental conditions, the predictions of the fraction of hydrocarbons with high chain length (>30) deviate from the experimental data. Although the overall chain growth factor (α_n) used in this study is intrinsically correlated with carbon number (n) due to the consideration of the re-adsorption of olefin products [15], the dependence of the chain growth rate on the carbon number is not completely taken into account. If one makes the kinetic parameters for propagation and termination rates to be a function of carbon number to consider the effect of steric hindrance due to the high chain length, the experimental data for high chain length will be predicted better. However, since the prediction of the amount of wax is beyond scope, this approach has not been conducted in this study.

CONCLUSIONS

A mathematical model for Fischer-Tropsch synthesis by an Fe-based catalyst has been developed and kinetic parameters have been estimated. Experimental data are produced by using a fixed-bed reactor under a variety of experimental conditions to make the data include a great deal of information about the dynamic behavior of a reactor and the distribution of hydrocarbon products. Estimation is conducted by fitting the experimental data, and the results show that the predicted values of CO conversion, methane selectivity, paraffin selectivity and the entire distribution of hydrocarbon products are in good agreement with the experimental data.

The developed model is used to evaluate the effect of operating conditions, and it is shown that the ratio of hydrogen to carbon monoxide in the feed mixture and the pressure play a key role in the determination of the entire distribution. Especially, the H_2/CO ratio is the most sensitive factor for the product quality in the sense that it increases the amount of light hydrocarbon and decreases both the amount of wax and the peak temperature inside the reactor. In conclusion, the developed model can be further used for the scale-up of a Fischer-Tropsch synthesis reactor and the determination of optimal operating conditions under which both maximum production rate and safe operation can be guaranteed.

ACKNOWLEDGMENT

The authors would like to acknowledge funding from the Korea Ministry of Knowledge Economy (MKE) through the Energy Technology Innovation Program. M.-J. Park acknowledges that this work was supported by the Korea Research Foundation Grant funded by the Korean Government (KRF-2008-313-D00202).

NOMENCLATURE

n : number of carbon
C_p : specific heat for the bulk gas phase [J/kg·K]
D_t : tube diameter, m
E_5 : activation energy of paraffin formation [kJ/mol] (n≥2)
E_{5M} : activation energy of methane formation [kJ/mol]
E_6 : activation energy of olefin formation [kJ/mol] (n≥2)
E_V : activation energy of WGS reaction [kJ/mol]
F_{obj} : objective function
$-\Delta H_2$: enthalpy of the hydrogenation of the adsorbed CO [kJ/mol]
$-\Delta H_3$: enthalpy of the hydrogenation of H-κ-C [kJ/mol]
$-\Delta H_4$: enthalpy of the hydrogenation of H-κ-CH_2 [kJ/mol]
$-\Delta H_v$: enthalpy of constants group in WGS reaction [kJ/mol]
$(-\Delta H)_j$: reaction heat of j th reaction [J/mol]
K_2 : equilibrium constant of the hydrogenation of the adsorbed CO

K_3 : equilibrium constant of the hydrogenation of H-κ-C
K_4 : equilibrium constant of the hydrogenation of H-κ-CH_2
K_v : group of constants in WGS reaction [$bar^{-0.5}$]
K_P : equilibrium constant of WGS reaction
N : maximum carbon number of the hydrocarbons involved
NR : total number of reaction involved
O_n : number-averaged chain length of olefins
O_w : weight-averaged chain length of olefins
P_i : partial pressure of component i [mol/s]
P_n : number-averaged chain length of paraffins
P_w : weight-averaged chain length of paraffins
R_j : overall reaction rate of reaction path j [mol/g·s]
T : temperature [K]
T_{in} : inlet temperature [K]
T_W : wall temperature [K]
U : overall heat transfer coefficient [$J/m^2 \cdot s \cdot K$]
X : CO conversion
c_i : concentration of component
k_1 : rate constant of CO adsorption [mol/g·s·bar]
$k_{1,0}$: pre-exponential factor of CO adsorption [mol/g·s·bar]
k_{5M} : rate constant of methane formation [mol/g·s·bar]
$k_{5M,0}$: pre-exponential factor of rate constant of methane formation [mol/g·s·bar]
k_5 : rate constant of paraffin formation [mol/g·s·bar]
$k_{5,0}$: pre-exponential factor of rate constant of paraffin formation [mol/g·s·bar] (n≥2)
k_6 : rate constant of olefin desorption reaction [mol/g·s]
$k_{6,0}$: pre-exponential factor of rate constant of olefin formation [mol/g·s] (n≥2)
k_v : rate constant of CO_2 formation [$mol/g \cdot s \cdot bar^{1.5}$]
$k_{v,0}$: pre-exponential factor of rate constant of CO_2 formation [$mol/g \cdot s \cdot bar^{1.5}$]
k_{-6} : rate constant of olefin re-adsorption reaction [mol/g·s·bar]
$k_{-6,0}$: pre-exponential factor of rate constant of olefin re-adsorption reaction [mol/g·s·bar]
u_S : gas velocity [m/s]
w_i : weighting factors
z : reactor dimension [m]

Greek Letters

α_1 : chain growth factor for carbon number of 1
α_{ij} : stoichiometric coefficient of component i in reaction j
α_n : chain growth factor for carbon number of n (n≥2)
α_A : chain growth probability in the Anderson-Schulz-Flory distribution
β_n : re-adsorption factor of 1-olefin with carbon number of n
κ : active site for FTS reactions
ρ_B : bulk pellet density [kg/m^3]
ρ_g : bulk gas density [kg/m^3]

REFERENCES

1. M. A. Vannice, *J. Catal.*, **37**, 449 (1975).
2. K. Eisenacher and A. A. Adesina, *Korean J. Chem. Eng.*, **17**, 71 (2000).
3. G. Zhao, C. Zhang, S. Qin, H. Xiang and Y. Li, *J. Mol. Catal. A: Chem.*, **286**, 137 (2008).
4. K. J. Yoon and E. J. Kim, *Korean J. Chem. Eng.*, **12**, 221 (1995).
5. K.-W. Jun, H.-S. Roh, K.-S. Kim, J.-S. Ryu and K.-W. Lee, *Appl. Catal. A-Gen.*, **259**, 221 (2004).
6. N. Lohitharn, J. G. Goodwin Jr. and E. Loterol, *J. Catal.*, **255**, 104 (2008).
7. S. Ledakowicz, H. Nettelhoff, R. Kokuun and W. D. Dekwer, *Ind. Eng. Chem. Process Des. Dev.*, **24**, 1043 (1985).
8. R. B. Anderson in Emmett, P. H. *Catalysis*, Rheinhold, New York (1956).
9. H. E. Atwood and C. O. Bennett, *Ind. Eng. Chem. Process Des. Dev.*, **18**, 163 (1979).
10. A. P. Raje and B. H. Davis, *Catal. Today*, **36**, 335 (1997).
11. G. A. Huff and C. N. Satterfield, *Ind. Eng. Chem. Process Des. Dev.*, **23**, 696 (1984).
12. M. E. Dry, T. Shingles and L. J. Boshoff, *J. Catal.*, **25**, 99 (1972).
13. W. H. Zimmerman, J. A. Rossin and D. B. Bukur, *Ind. Eng. Chem. Res.*, **28**, 406 (1989).
14. E. S. Lox and G. F. Froment, *Ind. Eng. Chem. Res.*, **32**, 71 (1993).
15. Y.-N. Wang, W.-P. Ma, Y.-J. Lu, J. Yang, Y.-Y. Xu, H. W. Xiang, Y.-W. Li, Y.-L. Zhao and B.-J. Zhang, *Fuel*, **82**, 195 (2003).
16. G. P. van der Laan and A. A. C. M. Beenackers, *Catal. Rev.-Sci. Eng.*, **41**, 255 (1999).
17. J. Yang, Y. Liu, J. Chang, Y.-N. Wang, L. Bai, Y.-Y. Xu, H.-W. Xiang, Y.-W. Li and B. Zhong, *Ind. Eng. Chem. Res.*, **42**, 5066 (2003).
18. J. De Deken, *De stoomreforming van methaan*, Doctoraatsthesis, Riksuniversiteit Gent (1982).
19. E. Akpan, Y. Sun, P. Kumar, H. Ibrahim, A. Aboudheir and R. Idem, *Chem. Eng. Sci.*, **62**, 4012 (2007).
20. R. A. Dictor and A. T. Bell, *J.Catal.*, **97**, 121 (1986).
21. J. L. Feimer, P. L. Silveston and R. R. Hudgins, *Ind. Eng. Chem. Prod. Res. Dev.*, **20**, 609 (1981).